

Pair excitations, collective modes, and gauge invariance in the BCS–Bose-Einstein crossover scenario

Ioan Kosztin, Qijin Chen, Ying-Jer Kao, and K. Levin

The James Franck Institute, The University of Chicago, 5640 South Ellis Avenue, Chicago, Illinois 60637

(Received 14 June 1999; revised manuscript received 11 October 1999)

In this paper we study the BCS Bose-Einstein condensation (BEC) crossover scenario within the superconducting state, using a T -matrix approach which yields the ground state proposed by Leggett. Here we extend this ground state analysis to finite temperatures T and interpret the resulting physics. We find two types of bosoniclike excitations of the system: long lived, incoherent pair excitations and collective modes of the superconducting order parameter, which have different dynamics. Using a gauge invariant formalism, this paper addresses their contrasting behavior as a function of T and superconducting coupling constant g . At a more physical level, our paper emphasizes how, at finite T , BCS-BEC approaches introduce an important parameter $\Delta_{pg}^2 = \Delta^2 - \Delta_{sc}^2$ into the description of superconductivity. This parameter is governed by the pair excitations and is associated with particle-hole asymmetry effects that are significant for sufficiently large g . In the fermionic regime, Δ_{pg}^2 represents the difference between the square of the excitation gap Δ^2 and that of the superconducting order parameter Δ_{sc}^2 . The parameter Δ_{pg}^2 , which is necessarily zero in the BCS (mean field) limit increases monotonically with the strength of the attractive interaction g . It follows that there is a significant physical distinction between this BCS-BEC crossover approach (in which g is the essential variable which determines Δ_{pg}) and the widely discussed phase fluctuation scenario in which the plasma frequency is the tuning parameter. Finally, we emphasize that in the strong coupling limit, there are important differences between the composite bosons that arise in crossover theories and the usual bosons of the (interacting) Bose liquid. Because of constraints imposed on the fermionic excitation gap and chemical potential, in crossover theories, the fermionic degrees of freedom can never be fully removed from consideration.

I. INTRODUCTION

The observation of an excitation gap above T_c (called the ‘‘pseudogap’’) in the underdoped cuprate superconductors has been the focus of much current research. An understanding of this state will help unravel the formal machinery, if not the attractive pairing mechanism behind high temperature superconductivity. It is now widely believed that this state is associated with the underlying superconducting phase, in large part because the (d -wave) symmetry of the pseudogap is found to be the same as that of the excitation gap and order parameter in the $T < T_c$ state.^{1,2} Among viable candidates for the origin of the pseudogap state are phase fluctuation scenarios,^{3,4} d -wave nodal excitation mechanisms⁵ and a BCS Bose-Einstein ‘‘crossover picture.’’^{6–17}

Here we discuss the last of these, the crossover scenario, within the superconducting state. Our work is directed towards the fundamental issues of the crossover problem, with lesser emphasis on the physics of the cuprates. We present a generalized overview based on a finite temperature T -matrix formulation. Our aim is to provide a useful understanding and to extend the physics of the well characterized ground state.¹⁸ In the process we establish a clear distinction between incoherent, finite center of mass momentum pair excitations and order parameter fluctuations (i.e., collective modes), and their respective dynamics. We formulate a gauge invariant description of the electrodynamic response with an emphasis on particle-hole asymmetry which is necessarily very important. Although we use a generalized

T -matrix approach, special attention will be paid to one particular version, called the ‘‘pairing approximation,’’ which has been extensively discussed in our previous work.^{9,11–13,19}

In the BCS Bose-Einstein condensation (BEC) crossover approach, it is presumed that there is a smooth evolution, with increasing attractive coupling constant g , from BCS superconductivity, in which strongly overlapping Cooper pairs form and Bose condense at precisely the same temperature T_c , to a quasi-ideal Bose gas state in which tightly bound fermion pairs (composite bosons) form at temperatures much higher than their Bose condensation temperature T_c . In this latter case there is an excitation gap for *fermionic* excitations well above T_c . This crossover picture dates back to Leggett,¹⁸ who, following earlier work by Eagles,²⁰ presented an interpolation scheme for the ground state based on a variational wave function. Shortly thereafter, Nozières and Schmitt-Rink²¹ (NSR) extended this theory to address finite T through calculations of T_c .

With the discovery of the short coherence length cuprates, several groups noted the relevance of this body of theoretical work. Randeria and co-workers²² reformulated the NSR approach and applied it to the cuprates. Micnas and co-workers^{23,7} presented detailed studies of the attractive Hubbard model and Uemura *et al.*¹⁰ noted, on the basis of unusual correlations deduced from muon spin resonance (μ SR) experiments, that the cuprates exhibited aspects of bosonic character, as might be expected in a crossover theory. Our own group¹² has also addressed cuprate issues in the past year using the formalism of the present paper.

Attempts to go beyond the NSR scheme at finite T are

relatively more recent and almost exclusively restricted to two-dimensional (2D) systems. These were motivated by the need to introduce a more self consistent treatment²⁴ of the pair and single-particle states. Numerical simulations^{25,26} on the attractive Hubbard model, along with numerical^{27,28} and analytical¹⁶ studies of the so-called FLEX (fluctuation exchange) scheme²⁹ have provided some insights. This diagrammatic FLEX approach should be contrasted with the alternative pairing approximation,^{9,11–13,19} which is based on earlier work by Kadanoff and Martin³⁰ and extended by Patton.³¹ In contrast to the FLEX scheme this latter approach precisely yields BCS theory in the small g limit. What is more important in distinguishing our work from that of others, however, is our direct focus^{11,12} on *crossover effects within the superconducting state*. This is the topic of the present paper, as well, and necessarily requires studies of systems in higher than two dimensions, where T_c is nonzero. The ultimately decisive factor in determining whether these crossover theories or any other alternatives are appropriate for the cuprates may well come from the predicted behavior below T_c . This fact has also been emphasized by Deutscher.³²

The assumptions of the BCS-BEC crossover theory need to be clearly stated. The starting point is a generic Hamiltonian describing fermions (with dispersion $\epsilon_{\mathbf{k}}$ measured from the chemical potential μ) in the presence of an attractive (spin-singlet) pairing interaction $V_{\mathbf{k},\mathbf{k}'}$. We assume a separable $V_{\mathbf{k},\mathbf{k}'} = g \varphi_{\mathbf{k}} \varphi_{\mathbf{k}'}$, with negative coupling constant g . The symmetry factor $\varphi_{\mathbf{k}}$ is to be associated with s - or d -wave pairing states. Moreover, it is assumed that (i) only two-body fermionic interactions are included. (ii) In calculations of *equilibrium* properties (as distinct from studies of the collective mode of the superconducting order parameter), repulsive Coulomb interactions between fermions are absorbed into the effective pairing interaction $V_{\mathbf{k},\mathbf{k}'}$. These Coulomb effects are presumed to be weak enough so that the attractive interactions driving superconductivity dominate, and it is assumed that Coulomb interactions do *not* occur between fermion pairs or composite bosons.

Using this Hamiltonian, Leggett¹⁸ found that, for arbitrary coupling g , the ground state wave function is given by the usual BCS form, where the two characteristic energy scales Δ and the fermionic chemical potential μ must be determined in a self consistent fashion. At $T=0$, in the weak coupling limit (where $\mu \approx E_F$), this scheme yields the usual BCS physics. By contrast, in the strong coupling (i.e., $g \rightarrow \infty$) limit, for the case of jellium, the system corresponds to a Bose condensation of nonoverlapping and *noninteracting* tightly bound pairs of fermions. This is an ‘‘essentially ideal Bose gas.’’²¹ Throughout this paper, we assume that ‘‘BCS-BEC crossover theory’’ is associated with this particular (Leggett) ground state.

II. PAIR EXCITATIONS IN BCS-BEC CROSSOVER THEORY: T -MATRIX BASED APPROACHES

A. Self-consistency conditions

In this section we introduce the concept of the pair excitation spectrum by extending the Leggett ground state to finite T . Quite generally, two important and interrelated effects ensue as the temperature is increased above $T=0$, and

the coupling g becomes sufficiently strong: (i) The excitation gap is no longer the same as (the amplitude of) the superconducting gap (order parameter). (ii) Incoherent pair excitations with nonzero center of mass momentum can be thermally excited. The pair excitation spectrum is associated with a pair propagator, called $\mathcal{T}(i\Omega, \mathbf{q})$. For nonzero $Q \equiv (i\Omega, \mathbf{q})$, we refer to this propagator as $\mathcal{T}_{pg}(Q)$, where the subscript pg derives from ‘‘pseudogap.’’ For small Ω and \mathbf{q} , it may be approximated by

$$\mathcal{T}_{pg}(i\Omega, \mathbf{q}) \approx a_0 / (i\Omega - \Omega_{\mathbf{q}} + i\Gamma_{\mathbf{q}} + \mu_{pair}), \quad (1)$$

where a_0 is the usual renormalization factor, $i\Omega$ is a bosonic Matsubara frequency, $\Omega_{\mathbf{q}}$ is the dispersion of the finite momentum pair excitations (with $\Omega_{\mathbf{q}=\mathbf{0}}=0$), $\Gamma_{\mathbf{q}}^{-1}$ is the pair excitation lifetime, and μ_{pair} is the effective pair ‘‘chemical potential.’’ As demonstrated in Appendix A, T -matrix-based schemes yield the ideal gas BEC condition

$$\mu_{pair} = 0 \quad \text{for} \quad T \leq T_c. \quad (2)$$

It should be stressed that within the BCS-BEC crossover picture, the form of \mathcal{T} is highly circumscribed so as to produce the correct ground state. Through the conditions on Δ and μ , the fermionic degrees of freedom play an important role, even at very strong coupling. As a consequence, the form for $\Omega_{\mathbf{q}}$ is also circumscribed. We find that the pairing approximation (discussed in Appendix A) produces the correct $T=0$ state and that, for sufficiently small \mathbf{q} , $\Omega_{\mathbf{q}} = \mathbf{q}^2 / 2M_{pair}$, where the pair mass M_{pair} is dependent on g , T , density n , lattice structure, and other materials properties.

We may now quantify point (i) listed above. The deviation between the excitation gap and the order parameter is related to the number of thermally excited finite momentum pair excitations. We define the difference between the excitation gap Δ and order parameter Δ_{sc} as $\Delta_{pg}^2 = \Delta^2 - \Delta_{sc}^2$, where throughout this paper, Δ_{sc} is taken to be real. The number of (incoherent) pair excitations, given in terms of the pair propagator \mathcal{T}_{pg} , is related to Δ_{pg} as

$$\Delta_{pg}^2 = - \sum_Q \mathcal{T}_{pg}(Q) = - \sum_Q \int_{-\infty}^{\infty} \frac{d\Omega}{\pi} b(\Omega) \text{Im} \mathcal{T}_{pg}(\Omega, \mathbf{q}), \quad (3)$$

where $b(\Omega)$ is the Bose function and $\mathcal{T}_{pg}(\Omega, \mathbf{q})$ is the analytically continued ($i\Omega \rightarrow \Omega + i0^+$) form of the pair propagator. Here and in what follows we use a four-vector notation $Q \equiv (i\Omega, \mathbf{q})$, $\Sigma_Q \equiv T \Sigma_{i\Omega} \Sigma_{\mathbf{q}}$, etc.

Equations (1)–(3) above are believed to be general to any T -matrix approach. Moreover, without specifying a microscopic formalism it is possible to anticipate a form for the coupled equations for Δ , Δ_{sc} , and μ subject to the following very reasonable constraints: these equations should be consistent (i) with the well established Leggett ground state, (ii) with BCS theory in the small g limit at all T , and finally (iii) with Eq. (3). One can readily write

$$g^{-1} + \sum_{\mathbf{k}} \frac{1 - 2f(E_{\mathbf{k}})}{2E_{\mathbf{k}}} \varphi_{\mathbf{k}}^2 = 0, \quad (4a)$$

where $E_{\mathbf{k}} = \sqrt{\epsilon_{\mathbf{k}}^2 + \Delta^2 \varphi_{\mathbf{k}}^2}$, and the number equation

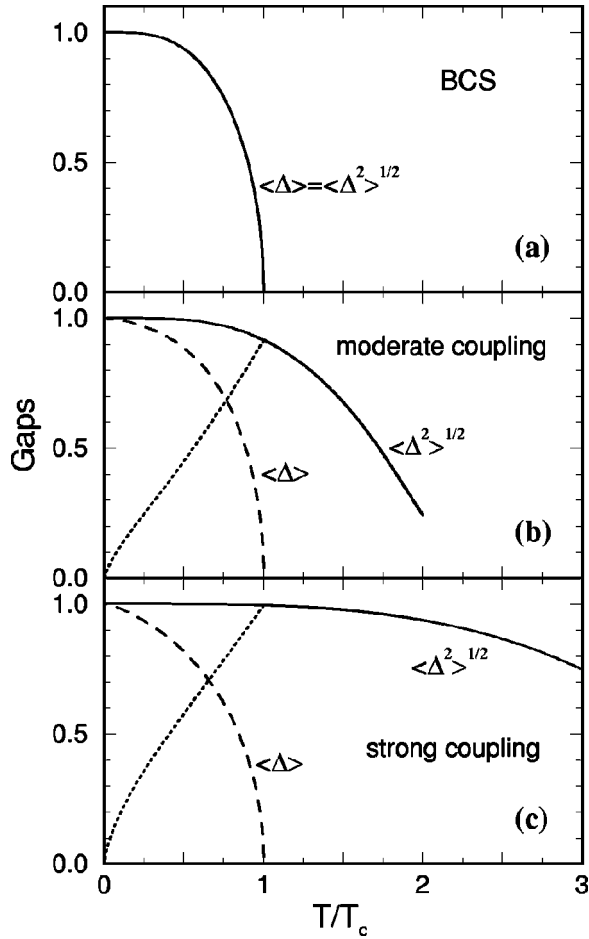


FIG. 1. Temperature dependence of the excitation gap $\langle \Delta^2 \rangle^{1/2} \equiv \Delta$ and the order parameter $\Delta_{sc} \equiv \langle \Delta \rangle$ (normalized at $T=0$) for (a) weak coupling BCS, (b) moderate coupling, and (c) strong coupling. The dotted lines represent the difference of these two energy scales, corresponding to the pseudogap parameter Δ_{pg} . A strong pseudogap develops as the coupling strength increases.

$$n = \sum_{\mathbf{k}} \left[1 - \frac{\epsilon_{\mathbf{k}}}{E_{\mathbf{k}}} + \frac{2\epsilon_{\mathbf{k}}}{E_{\mathbf{k}}} f(E_{\mathbf{k}}) \right]. \quad (4b)$$

Finally, the decomposition of Δ into Δ_{sc} and Δ_{pg} requires the solution of the third equation, namely Eq. (3) which we rewrite as

$$\Delta^2 - \Delta_{sc}^2 = \Delta_{pg}^2 = a_0 \sum_{\mathbf{q} \neq 0} b(\Omega_{\mathbf{q}}), \quad (4c)$$

where only the parameters a_0 and $\Omega_{\mathbf{q}}$ depend on the particular microscopic T -matrix scheme.

B. Comparison with phase fluctuation scenario

Using Eqs. (4), the behavior of Δ_{pg} , Δ , and Δ_{sc} is computed and the results plotted in Fig. 1 in the three different regimes: weak (BCS), intermediate, and strong coupling (nearly BEC) regimes. Below T_c these plots are based on detailed numerical calculations,¹¹ whereas above T_c , where the computations are more difficult,¹³ on a simple extrapolation procedure.³³

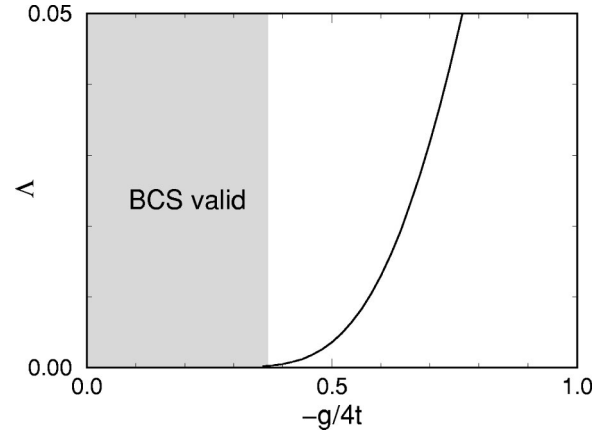


FIG. 2. Dependence of the cutoff momentum Λ (where the pair excitation spectrum crosses into the particle-particle continuum), on the coupling strength on a quasi-2D lattice. Here $4t$ is the half bandwidth. Because of strong damping of the pair excitations, they are irrelevant at low g and BCS theory is valid in the shaded region. Outside this regime, pair excitations become important.

It may be noted that Fig. 1 has a direct analog in the phase fluctuation scenario.³ The three panels (from top to bottom) would then correspond to progressively decreasing the size of the *phase stiffness*³ parameter, called n/m^* . In this phase fluctuation scenario the tuning parameter is n/m^* , whereas in the crossover scenario the coupling constant g sets the scale for the size of Δ_{pg}^2 . Moreover, the important dynamics of the phase fluctuation scenario derives from the fluctuations in the order parameter whereas, in the present crossover scenario, the dynamical energy scale corresponds to the pair excitation spectrum $\Omega_{\mathbf{q}}$. The crossover approach should be viewed as a *mean-field*-based scheme which, even in the absence of fluctuations, introduces a distinction between Δ and Δ_{sc} .

It should, finally, be stressed that these incoherent, finite momentum pair excitations are irrelevant in the BCS limit, in accord with Fig. 1(a). In that limit the “quasiparticle” assumption implicit in Eq. (1) is invalid and because of both the lack of particle-hole asymmetry and the large damping $\Gamma_{\mathbf{q}}$, the pair excitation spectrum merges with the particle-particle continuum. One can quantify the reliability of this key approximation. In Fig. 2, using our numerical scheme,¹² we plot the value Λ of the wave vector $|\mathbf{q}|$ at which the pair dispersion intersects the continuum states, as a function of coupling g . This corresponds to a measure of the Landau damping of the pair propagator. The shaded region indicates where the incoherent finite momentum pairs represent ill-defined excitations. Outside this shaded region, the assumptions implicit in Eq. (1) should be valid. Related calculations show that $\Delta_{pg}(T_c)/\Delta_{sc}(0)$ is arbitrarily small in the weak coupling limit, so that even if we apply Eq. (1) directly in this limit, pseudogap effects are negligible in the BCS regime.

C. Comparison between the bosons of the strong coupling limit and “true” bosons

A first important distinction can be found, between the composite bosons of the present theory and “true” bosons, at the level of the Leggett ground state. From previous work

at $T=0$ in the strong coupling limit, it can be seen that this ground state contains a mix of quasi-ideal and interacting Bose gas character. The gap equation is associated¹⁸ with “noninteracting diatomic molecules,” whereas, the collective mode spectrum^{34–36} reflects an effective boson-boson interaction deriving from the Pauli statistics of the constituent fermions. This is seen most clearly in jellium models where the Anderson-Bogoliubov (AB) sound velocity remains finite at infinite g , with an asymptote associated with these residual interactions.^{8,37}

For large g , this “boson-boson repulsion” derives entirely from Fermi statistical effects. In contrast to the true interacting Bose system,³⁸ where boson-boson interactions need to be separately included in the boson propagator, here the physics associated with the Pauli principle is already accounted for and should not be fed back again to renormalize the dispersion of composite bosons.

A second important difference between true and composite bosons arises from the fact that this superconducting ground state corresponds to one in which there is full condensation so that, as in the BCS phase, the condensate fraction $n_0 = n$. By contrast, in a Bose superfluid there is always a depletion of the condensate at $T=0$, caused by the existence of an interboson repulsion.

As a final important difference, we note that the behavior of the pair propagator \mathcal{T} , which must necessarily be consistent with the $T=0$ gap and number equations,¹⁸ is highly circumscribed and rather different from what one might deduce based on the standard model for a Bose liquid.³⁸ The fermionic degrees of freedom can never be fully “integrated out.” The fermionic excitation gap Δ and the pair chemical potential $\mu_{pair}=0$ are, moreover, closely interrelated via, e.g., Eq. (A4) in Appendix A. These effects have no natural counterpart in the Bose liquid (where the fermionic excitation gap is of no consequence).

III. ELECTROMAGNETIC RESPONSE AND COLLECTIVE MODES OF A SUPERCONDUCTOR: BEYOND BCS THEORY

The purpose of this section is to study the gauge invariant (linear) response of a superconductor to an external electromagnetic (EM) field, and obtain the associated collective mode spectrum. Our discussion is generally relevant to complex situations such as those appropriate to the BCS-BEC crossover scenario. An important ingredient of this discussion is establishing the role of particle-hole asymmetry. It should be noted that there are fairly extensive discussions in the literature on the behavior of collective modes within the $T=0$ crossover scenario.^{34–36,39} Here we review a slightly different formulation^{40,41} that introduces a matrix extension of the Kubo formalism of the normal state. We find that this approach is more directly amenable to extension to finite T , where the pair fluctuation diagrams need to be incorporated.

The definition of the collective modes of a superconductor must be made with some precision. We refer to the underlying Goldstone boson of the charged or uncharged superconductor as the “AB mode,” after Anderson⁴² and Bogoliubov.⁴³ This AB mode appears as a pole structure in the gauge invariant formulation of the electrodynamic response functions, for example, in the density-density corre-

lation function. Early work by Prange⁴⁴ referred to this as the “ghost mode” of the neutral system, since this term is not directly affected by the long range Coulomb interaction. By contrast, the normal modes of the charged or uncharged superconductor, which we shall call the “collective modes,” involve a coupling between the density, phase, and for the BCS-BEC case, amplitude degrees of freedom. For these, one needs to incorporate a many-body theoretic treatment of the particle-hole channel as well. In crossover theories this channel is not as well characterized as is the particle-particle channel.

A. Gauge invariant EM response kernel

In the presence of a weak externally applied EM field, with four-vector potential $A^\mu = (\phi, \mathbf{A})$, the four-current density $J^\mu = (\rho, \mathbf{J})$ is given by

$$J^\mu(Q) = K^{\mu\nu}(Q)A_\nu(Q), \quad (5)$$

where, $Q \equiv q^\mu = (\omega, \mathbf{q})$ is a four-momentum, and $K^{\mu\nu}$ is the EM response kernel, which can be written as

$$K^{\mu\nu}(Q) = K_0^{\mu\nu}(Q) + \delta K^{\mu\nu}(Q). \quad (6)$$

Here

$$K_0^{\mu\nu}(\omega, \mathbf{q}) = P^{\mu\nu}(\omega, \mathbf{q}) + \frac{ne^2}{m} g^{\mu\nu} (1 - g^{\mu 0}) \quad (7)$$

is the usual Kubo expression for the electromagnetic response. We define the current-current correlation function $P^{\mu\nu}(\tau, \mathbf{q}) = -i\theta(\tau)\langle [j^\mu(\tau, \mathbf{q}), j^\nu(0, -\mathbf{q})] \rangle$. In the above equation, $g^{\mu\nu}$ is the contravariant diagonal metric tensor, with diagonal elements $(1, -1, -1, -1)$, and n , e , and m are the particle density, charge, and mass, respectively. In what follows, we will set $e=1$ for simplicity.

The presence of $\delta K^{\mu\nu}$ in Eq. (6) is due to the perturbation of the superconducting order parameter by the EM field, i.e., to the excitation of the *collective modes* of Δ_{sc} . This term is required to satisfy charge conservation $q_\mu J^\mu = 0$, which requires that

$$q_\mu K^{\mu\nu}(Q) = 0. \quad (8a)$$

Moreover, gauge invariance yields

$$K^{\mu\nu}(Q)q_\nu = 0, \quad (8b)$$

Note that, since $K^{\mu\nu}(-Q) = K^{\nu\mu}(Q)$, the two constraints Eqs. (8) are in fact equivalent.

The incorporation of gauge invariance into a general microscopic theory may be implemented in several ways. Here we do so via a general matrix linear response approach⁴⁰ in which the perturbation of the condensate is included as additional contributions $\Delta_1 + i\Delta_2$ to the applied external field. These contributions are self consistently obtained (by using the gap equation) and then eliminated from the final expression for $K^{\mu\nu}$. We now implement this procedure. Let $\eta_{1,2}$ denote the change in the expectation value of the pairing field $\hat{\eta}_{1,2}$ corresponding to $\Delta_{1,2}$. For the case of an s -wave pairing interaction $g < 0$, the self-consistency condition $\Delta_{1,2} = g\eta_{1,2}/2$ leads to the following equations:

$$J^\mu = K^{\mu\nu} A_\nu = K_0^{\mu\nu} A_\nu + R^{\mu 1} \Delta_1 + R^{\mu 2} \Delta_2, \quad (9a)$$

$$\eta_1 = -\frac{2\Delta_1}{|g|} = R^{1\nu} A_\nu + Q_{11} \Delta_1 + Q_{12} \Delta_2, \quad (9b)$$

$$\eta_2 = -\frac{2\Delta_2}{|g|} = R^{2\nu} A_\nu + Q_{21} \Delta_1 + Q_{22} \Delta_2, \quad (9c)$$

where $R^{\mu i}(\tau, \mathbf{q}) = -i\theta(\tau)\langle [j^\mu(\tau, \mathbf{q}), \hat{\eta}_i(0, -\mathbf{q})] \rangle$, with $\mu = 0, \dots, 3$, and $i = 1, 2$; and

$$Q_{ij}(\tau, \mathbf{q}) = -i\theta(\tau)\langle [\hat{\eta}_i(\tau, \mathbf{q}), \hat{\eta}_j(0, -\mathbf{q})] \rangle,$$

with $i, j = 1, 2$.

Thus far, the important quantities $K_0^{\mu\nu}$, $R^{\mu i}$ and Q_{ij} are unknowns that contain the details of the appropriate micro-

scopic model. We shall return to these later in Sec. IV. The last two of Eqs. (9) can be used to express $\Delta_{1,2}$ in terms of A_ν :

$$\Delta_1 = -\frac{\tilde{Q}_{22}R^{1\nu} - Q_{12}R^{2\nu}}{\tilde{Q}_{11}\tilde{Q}_{22} - Q_{12}Q_{21}} A_\nu, \quad (10a)$$

$$\Delta_2 = -\frac{\tilde{Q}_{11}R^{2\nu} - Q_{21}R^{1\nu}}{\tilde{Q}_{11}\tilde{Q}_{22} - Q_{12}Q_{21}} A_\nu, \quad (10b)$$

where $\tilde{Q}_{ii} = 2|g| + Q_{ii}$, with $i = 1, 2$. Finally, inserting Eqs. (10) into Eq. (9a) one obtains

$$K^{\mu\nu} = K_0^{\mu\nu} + \delta K^{\mu\nu}, \quad (11a)$$

with

$$\delta K^{\mu\nu} = -\frac{\tilde{Q}_{11}R^{\mu 2}R^{2\nu} + \tilde{Q}_{22}R^{\mu 1}R^{1\nu} - Q_{12}R^{\mu 1}R^{2\nu} - Q_{21}R^{\mu 2}R^{1\nu}}{\tilde{Q}_{11}\tilde{Q}_{22} - Q_{12}Q_{21}}. \quad (11b)$$

As can be seen from the above rather complicated equation, the electromagnetic response of a superconductor involves many different components of the generalized polarizability. Moreover, in the form of Eq. (11b) it is not evident that the results are gauge invariant. In order to demonstrate gauge invariance and reduce the number of component polarizabilities, we first rewrite $K^{\mu\nu}$ in a way which incorporates the effects of the amplitude contributions via a renormalization of the relevant generalized polarizabilities, i.e.,

$$K^{\mu\nu} = K'^{\mu\nu} + \delta K'^{\mu\nu}, \quad (12a)$$

where

$$K'^{\mu\nu} = K_0^{\mu\nu} - \frac{R^{\mu 1}R^{1\nu}}{\tilde{Q}_{11}} \quad (12b)$$

and

$$R'^{\mu 2} = R^{\mu 2} - \frac{Q_{12}}{\tilde{Q}_{11}} R^{\mu 2}, \quad \tilde{Q}'_{22} = \tilde{Q}_{22} - \frac{Q_{12}Q_{21}}{\tilde{Q}_{11}}. \quad (12c)$$

In this way we obtain a simpler expression for $\delta K'^{\mu\nu}$:

$$\delta K'^{\mu\nu} = -\frac{R'^{\mu 2}R'^{2\nu}}{\tilde{Q}'_{22}}. \quad (13)$$

We now consider a particular (*a priori* unknown) gauge A'^μ in which the current density can be expressed as $J^\mu = K'^{\mu\nu} A'_\nu$. The gauge transformation⁴⁵ that connects the four-potential A_μ in an arbitrary gauge with A'_μ , i.e., $A'_\mu = A_\mu + i\chi q_\mu$, must satisfy

$$J^\mu = K^{\mu\nu} A_\nu = K'^{\mu\nu} (A'_\nu + i\chi q_\nu). \quad (14)$$

Now invoking charge conservation, one obtains

$$i\chi = -\frac{q_\mu K'^{\mu\nu} A'_\nu}{q_{\mu'} K'^{\mu'\nu'} q_{\nu'}}, \quad (15)$$

and, therefore,

$$K^{\mu\nu} = K'^{\mu\nu} - \frac{(K'^{\mu\nu'} q_{\nu'})(q_{\nu''} K'^{\nu''\nu})}{q_{\mu'} K'^{\mu'\nu'} q_{\nu'}}. \quad (16)$$

The above equation satisfies two important requirements: it is manifestly gauge invariant and, moreover, it has been reduced to a form that depends principally on the four-current-current correlation functions. [The word ‘‘principally’’ appears because in the absence of particle-hole symmetry, there are effects associated with the order parameter amplitude contributions that enter via Eq. (12) and add to the complexity of the calculations.] Equation (16) should be directly compared with Eq. (11b). In order for the formulations to be consistent and to explicitly keep track of the conservation laws (8), the following identities must be satisfied:

$$(q_\mu K'^{\mu\nu}) \tilde{Q}'_{22} = (q_\mu R'^{\mu 2}) R'^{2\nu}, \quad (17a)$$

$$(K'^{\mu\nu} q_\nu) \tilde{Q}'_{22} = R'^{\mu 2} (R'^{2\nu} q_\nu). \quad (17b)$$

These identities may be viewed as ‘‘Ward identities’’ for the superconducting two-particle correlation functions.⁴¹ Any theory that adds additional self-energy contributions to the BCS scheme must obey these important equations. We shall return to this issue in Sec. IV.

B. The Goldstone boson or AB mode

The EM response kernel [cf. Eqs. (12)–(16)] of a superconductor contains a pole structure that is related to the underlying Goldstone boson of the system. Unlike the phase mode component of the collective mode spectrum, this AB

mode is independent of Coulomb effects.⁴⁴ The dispersion of this amplitude renormalized AB mode is given by

$$q_\mu K_0^{\prime\mu\nu} q_\nu = 0. \quad (18)$$

For an isotropic system $K_0^{\prime\alpha\beta} = K_0^{\prime11} \delta_{\alpha\beta}$, and Eq. (18) can be rewritten as

$$\omega^2 K_0^{\prime00} + \mathbf{q}^2 K_0^{\prime11} - 2\omega q_\alpha K_0^{\prime0\alpha} = 0, \quad (19)$$

with $\alpha = 1, 2, 3$, and in the last term on the left-hand side of Eq. (19) a summation over repeated Greek indices is assumed. It might seem surprising that from an analysis which incorporates a complicated matrix linear response approach, the dispersion of the AB mode ultimately involves only the amplitude renormalized four-current correlation functions, namely the density-density, current-current, and density-current correlation functions. This result is, nevertheless, a consequence of gauge invariance.

At zero temperature $K_0^{\prime0\alpha}$ vanishes, and the soundlike AB mode has the usual linear dispersion $\omega = \omega_{\mathbf{q}} = c|\mathbf{q}|$ with the ‘‘sound velocity’’ given by

$$c^2 = K_0^{\prime11}/K_0^{\prime00}. \quad (20)$$

The equations in this section represent an important starting point for our numerical analysis.

C. General collective modes

We may interpret the AB mode as a special type of collective mode which is associated with $A_\nu = 0$ in Eqs. (10). This mode corresponds to free oscillations of $\Delta_{1,2}$ with a dispersion $\omega = cq$ given by the solution to the equation

$$\det|Q_{ij}| = \tilde{Q}_{11}\tilde{Q}_{22} - Q_{12}Q_{21} = 0. \quad (21)$$

More generally, according to Eq. (9a) the collective modes of the order parameter induce density and current oscillations. In the same way as the pairing field couples to the mean-field order parameter in the particle-particle channel, the density operator $\hat{\rho}(Q)$ couples to the mean field $\delta\phi(Q) = V(Q)\delta\rho(Q)$, where $V(Q)$ is an effective particle-hole interaction that may derive from the pairing channel or, in a charged superconductor, from the Coulomb interaction. Here $\delta\rho = \langle\hat{\rho}\rangle - \rho_0$ is the expectation value of the charge density operator with respect to its uniform, equilibrium value ρ_0 . Within our self-consistent linear response theory the field $\delta\phi$ must be treated on an equal footing with $\Delta_{1,2}$ and formally can be incorporated into the linear response of the system by adding an extra term $K_0^{\mu0}\delta\phi$ to the right hand side of Eq. (9a). The other two Eqs. (9) should be treated similarly. Note that, quite generally, the effect of the ‘‘external field’’ $\delta\phi$ amounts to replacing the scalar potential $A^0 = \phi$ by $\bar{A}^0 = \bar{\phi} = \phi + \delta\phi$. In this way one arrives at the following set of three linear, homogeneous equations for the unknowns $\delta\phi$, Δ_1 , and Δ_2

$$0 = R^{10}\delta\phi + \tilde{Q}_{11}\Delta_1 + Q_{12}\Delta_2, \quad (22a)$$

$$0 = R^{20}\delta\phi + Q_{21}\Delta_1 + \tilde{Q}_{22}\Delta_2, \quad (22b)$$

$$\delta\rho = \frac{\delta\phi}{V} = K_0^{00}\delta\phi + R^{01}\Delta_1 + R^{02}\Delta_2. \quad (22c)$$

The dispersion of the collective modes of the system is given by the condition that the above Eqs. (22) have a nontrivial solution

$$\begin{vmatrix} Q_{11} + 2/|g| & Q_{12} & R^{10} \\ Q_{21} & Q_{22} + 2/|g| & R^{20} \\ R^{01} & R^{02} & K_0^{00} - 1/V \end{vmatrix} = 0. \quad (23)$$

In the case of particle-hole symmetry $Q_{12} = Q_{21} = R^{10} = R^{01} = 0$ and, the amplitude mode decouples from the phase and density modes; the latter two are, however, in general coupled.

IV. EFFECT OF PAIR FLUCTUATIONS ON THE ELECTROMAGNETIC RESPONSE: SOME EXAMPLES

Once dressed Green’s functions G enter into the calculational schemes, the collective mode polarizabilities (e.g., Q_{22}) and the EM response tensor $K_0^{\mu\nu}$ must necessarily include vertex corrections dictated by the form of the self-energy Σ , which depends on the T matrix \mathcal{T} , which, in turn depends on the form of the pair susceptibility χ defined in Appendix A. These vertex corrections are associated with gauge invariance and with the constraints that are summarized in Eqs. (17). It can be seen that these constraints are even more complicated than the Ward identities of the normal state. Indeed, it is relatively straightforward to introduce collective mode effects into the electromagnetic response in a completely general fashion that is required by gauge invariance. This issue was discussed in Sec. III as well as extensively in the literature.^{46,36} The difficulty is in the implementation. In this section we begin with a discussion of the $T = 0$ behavior where the incoherent pair excitation contributions to the self-energy corrections and vertex functions vanish. In this section, we shall keep the symmetry factor $\varphi_{\mathbf{k}}$ explicitly.

A. $T=0$ behavior of the AB mode and pair susceptibility

It is quite useful to first address the zero temperature results since there it is relatively simple to compare the associated polarizabilities of the AB mode with that of the pair susceptibility χ . In the presence of particle-hole symmetry this collective mode polarizability can be associated with Q_{22} , which was first defined in Eq. (9c). In the more general case (which applies away from the BCS limit) Q_{22} must be replaced by a combination of phase and amplitude terms so that it is given by $Q'_{22} = Q_{22} - Q_{12}Q_{21}/\tilde{Q}_{11}$.

We may readily evaluate these contributions in the ground state, where $\Delta_{sc} = \Delta$. The polarizability Q_{22} is given by

$$Q_{22}(Q) = - \sum_P [G(-P)G(P-Q) + G(P)G(Q-P) + F^\dagger(P)F^\dagger(P-Q) + F(P)F(P-Q)]\varphi_{\mathbf{P}-\mathbf{Q}}^2, \quad (24)$$

where

$$G(K) = G_0(K) / [1 + \Delta_{sc}^2 \varphi_{\mathbf{k}}^2 G_0(-K) G_0(K)], \quad (25)$$

and

$$F(P) = \Delta_{sc} \varphi_{\mathbf{p}} G(P) G_0(-P). \quad (26)$$

Now, it can be seen that the pair susceptibility χ in the pairing approximation satisfies

$$\begin{aligned} & \sum_P [G(-P)G(P) + F(P)F(P)] \varphi_{\mathbf{p}}^2 \\ &= \sum_P G(P)G_0(-P) \varphi_{\mathbf{p}}^2 = \chi(0), \end{aligned} \quad (27)$$

and, moreover, $Q_{12}(0) = Q_{21}(0) = 0$ so that

$$\frac{2}{|g|} + Q_{22}(0) = \frac{2}{|g|} [1 + g\chi(0)] = 0. \quad (28)$$

In this way, the AB mode propagator is soft under the same conditions which yield a soft pair excitation propagator $\mathcal{T}_{pg} = g/(1 + g\chi)$, and these conditions correspond to the gap equation Eq. (4a) at $T=0$. Moreover, it can be seen that $Q'_{22}(Q) = Q'_{22}(-Q)$ so that, upon expanding around $Q=0$, one has $\tilde{Q}_{22}(Q) = -\alpha_{22}\Omega^2 + \beta_{22}Q^2$, $Q_{12}(Q) = -Q_{21}(Q) = i\Omega\alpha_{12}$, and $2/|g| + Q_{11}(Q) = 2/|g| - \alpha_{11}$, where

$$\begin{aligned} \alpha_{22} &= \sum_{\mathbf{k}} \frac{\varphi_{\mathbf{k}}^2}{4E_{\mathbf{k}}^3}, \\ \beta_{22} &= \frac{1}{d} \sum_{\mathbf{k}} \frac{1}{4E_{\mathbf{k}}^3} \left[\varphi_{\mathbf{k}}^2 (\nabla \epsilon_{\mathbf{k}})^2 - \frac{1}{4} (\nabla \epsilon_{\mathbf{k}}^2) \cdot (\nabla \varphi_{\mathbf{k}}^2) \right], \\ \alpha_{12} &= \sum_{\mathbf{k}} \frac{\epsilon_{\mathbf{k}}}{2E_{\mathbf{k}}^3} \varphi_{\mathbf{k}}^2, \\ \alpha_{11} &= \sum_{\mathbf{k}} \frac{\epsilon_{\mathbf{k}}^2}{E_{\mathbf{k}}^3} \varphi_{\mathbf{k}}^2, \end{aligned} \quad (29)$$

where d denotes the dimensionality of the system. Thus, one obtains

$$c^2 = \frac{\beta_{22}}{\alpha_{12}^2 + \frac{2}{|g|} - \alpha_{11}}. \quad (30)$$

At weak coupling in three dimensions, where one has particle-hole symmetry, $\alpha_{12} = 0$, the amplitude and the phase modes decouple. This leads to the well-known result $c = v_F/\sqrt{3}$. More generally, for arbitrary coupling strength g , these equations yield results equivalent to those in the literature,^{34–36,39} as well as those derived from the formalism of Sec. III B. Finally, it should be noted that since both Eqs. (16) and (13) have the same poles, the condition $\tilde{Q}'_{22}(Q) = 0$ yields the same AB mode dispersion as that determined from Eq. (18). This is a consequence of gauge invariance.

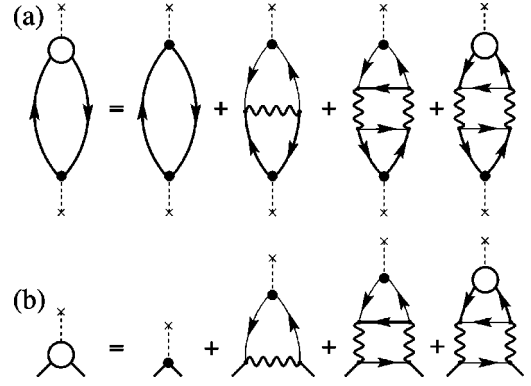


FIG. 3. Diagrammatic representation of (a) the polarization bubble and (b) the vertex function used to compute the electrodynamic response functions. Here the wavy lines represent \mathcal{T} and it should be noted that the thin and thick lines correspond to G_0 and G respectively. The total vertex correction is given by the sum of the Maki Thompson (MT) and two Aslamazov-Larkin (AL_1 and AL_2) diagrams.

B. AB mode at finite temperatures

We now turn to finite temperatures where there is essentially no prior work on the collective mode behavior in the crossover scenario. At the level of BCS theory (and in the Leggett ground state) the extended “Ward identities” of Eqs. (17) can be explicitly shown to be satisfied. Presumably they are also obeyed in the presence of impurities, as, for example, in the scheme of Ref. 40. However, in general, it is difficult to go beyond these simple cases in computing all components of the matrix response function. Fortunately, the calculation of the AB mode is somewhat simpler. It reduces to a solution of Eq. (19), which, *in the presence of particle-hole symmetry*, involves a computation of only the electromagnetic response kernel: the density-density, density-current and current-current correlation functions.

It is the goal of this section to compute these three response functions within the “pairing approximation” to the T matrix. Our work is based on the normal state approach of Patton³¹ and the associated diagrams are shown in Fig. 3. Because full Green’s functions G appear in place of G_0 (as indicated by the heavy lines) these diagrams are related to but different³¹ from their counterparts studied by Aslamazov and Larkin and by Maki and Thompson. This diagram scheme forms the basis for calculations published by our group^{11,19} of the penetration depth within the BCS-BEC crossover scheme.

Here we make one additional assumption. We treat the amplitude renormalizations that appear in Eqs. (12) only approximately, since these contributions introduce a variety of additional correlation functions, which must be calculated in a consistent fashion, so as to satisfy Eqs. (17). Because the amplitude mode is gapped, at least at low T , we can approximate these amplitude renormalizations by their $T=0$ counterparts, which are much simpler to deduce.

The three electromagnetic correlation functions reduce to a calculation of $P^{\mu\nu}$, which can be written as

$$P^{\mu\nu}(Q) = 2 \sum_K \lambda^{\mu}(K, K-Q) G(K) G(K-Q) \Lambda^{\nu}(K, K-Q), \quad (31)$$

where

$$\lambda(K, K-Q) = (1, \nabla_{\mathbf{k}} \epsilon_{\mathbf{k}-\mathbf{q}/2})$$

and

$$\Lambda(K, K-Q) = \lambda(K, K-Q) + \delta\Lambda_{sc}(K, K-Q) + \delta\Lambda_{pg}(K, K-Q)$$

are the bare and full vertices, respectively.

To evaluate the vertex function Λ^μ we decompose it into a pseudogap contribution Λ_{pg} and a superconducting contribution Λ_{sc} . (The latter can be regarded as the Gor'kov F function contribution, although we do not use that notation here). The pseudogap contribution comes from a sum of Maki-Thompson (MT) and Aslamazov-Larkin (AL_{1,2}) diagrams [see Fig. 3(b)]. Since these vertex corrections can be obtained from a proper vertex insertion to the self-energy, it follows that there is a cancellation between these various terms that simplifies the algebra. This cancellation is shown in more detail in Appendix B. Following the analysis in Appendix B, the sum of both pg and sc contributions is given by

$$\begin{aligned} \delta\Lambda^\mu(K, K-Q) &\approx -(\Delta_{sc}^2 - \Delta_{pg}^2) \varphi_{\mathbf{k}} \varphi_{\mathbf{k}-\mathbf{q}} G_0(-K) G_0 \\ &\quad \times (Q-K) \lambda^\mu(Q-K, -K) \\ &\quad - \Delta_{pg}^2 G_0(-K) \frac{\partial \varphi_{\mathbf{k}-\mathbf{q}/2}^2}{\partial k_\mu}, \end{aligned} \quad (32)$$

where use has been made of the fact that $\mathcal{T}_{pg}(Q)$ is highly peaked at $Q=0$, and that $\Delta_{pg}^2 \equiv -\sum_Q \mathcal{T}_{pg}(Q)$.

The AB mode dispersion involves the sum of three terms that enter into Eqs. (18) and (19). We next substitute Eq. (32) into Eq. (31). After performing the Matsubara frequency summation, and analytically continuing $i\Omega \rightarrow \Omega + i0^+$, we obtain for small Ω and \mathbf{q}

$$\begin{aligned} q_\mu K_0^{\mu\nu} q_\nu &= \mathbf{q} \cdot \left(\frac{\tilde{\mathbf{n}}}{\mathbf{m}} + \vec{\mathbf{P}} \right) \cdot \mathbf{q} - 2\Omega \mathbf{q} \cdot \mathbf{P}_0 + \Omega^2 P_{00} \\ &= \frac{2}{d} q^2 \sum_{\mathbf{k}} \frac{\Delta_{sc}^2}{E_{\mathbf{k}}^2} \left[\frac{1-2f(E_{\mathbf{k}})}{2E_{\mathbf{k}}} + f'(E_{\mathbf{k}}) \right] \\ &\quad \times \left[\varphi_{\mathbf{k}}^2 (\vec{\nabla} \epsilon_{\mathbf{k}})^2 - \frac{1}{4} (\vec{\nabla} \epsilon_{\mathbf{k}}^2) \cdot (\vec{\nabla} \varphi_{\mathbf{k}}^2) \right] \\ &\quad - 2\Omega^2 \sum_{\mathbf{k}} \left\{ \frac{\Delta_{sc}^2 \varphi_{\mathbf{k}}^2}{E_{\mathbf{k}}^2} \left[\frac{1-2f(E_{\mathbf{k}})}{2E_{\mathbf{k}}} + f'(E_{\mathbf{k}}) \right] \right. \\ &\quad \left. - f'(E_{\mathbf{k}}) \frac{\Omega^2 - (\mathbf{q} \cdot \vec{\nabla} \epsilon_{\mathbf{k}})^2 - \Delta^2 (\mathbf{q} \cdot \vec{\nabla} \varphi_{\mathbf{k}})^2}{\Omega^2 - (\mathbf{q} \cdot \vec{\nabla} E_{\mathbf{k}})^2} \right\} \\ &\quad + \frac{\Delta_{pg}^2}{4E_{\mathbf{k}}^2} f'(E_{\mathbf{k}}) \frac{(\mathbf{q} \cdot \nabla \epsilon_{\mathbf{k}}^2) (\mathbf{q} \cdot \vec{\nabla} \varphi_{\mathbf{k}}^2) + \Delta^2 (\mathbf{q} \cdot \vec{\nabla} \varphi_{\mathbf{k}}^2)^2}{\Omega^2 - (\mathbf{q} \cdot \vec{\nabla} E_{\mathbf{k}})^2} \Bigg\}, \end{aligned} \quad (33)$$

where $f(E)$ is the Fermi function. Because Eq. (33) is ill-behaved for long wavelengths and low frequencies, in order to calculate the AB mode velocity one needs to take the

appropriate limit $\Omega = cq \rightarrow 0$. By contrast, the calculation of the London penetration depth first requires setting $\Omega = 0$ (static limit), and then $\mathbf{q} \rightarrow 0$. The superfluid density n_s can be calculated from the coefficient of the q^2 term in Eq. (33) [see, also Eq. (C1) for $Q=0$]. Finally, the AB mode ‘‘sound’’ velocity $c = \Omega/q$, in the absence of the amplitude renormalization, can be obtained by solving $q_\mu K_0^{\mu\nu} q_\nu = 0$.

In the absence of the pseudogap (i.e., when $\Delta_{sc} = \Delta$) the last term inside $\{\dots\}$ in Eq. (33) drops out, and the resulting analytical expression reduces to the standard BCS result,⁴⁷ which at $T=0$ has the relatively simple form

$$\begin{aligned} q_\mu K_0^{\mu\nu} q_\nu &= \frac{q^2}{d} \sum_{\mathbf{k}} \frac{\Delta_{sc}^2}{E_{\mathbf{k}}^3} \left[\varphi_{\mathbf{k}}^2 (\nabla \epsilon_{\mathbf{k}})^2 - \frac{1}{4} (\nabla \epsilon_{\mathbf{k}}^2) \cdot (\nabla \varphi_{\mathbf{k}}^2) \right] \\ &\quad - \Omega^2 \sum_{\mathbf{k}} \frac{\Delta_{sc}^2 \varphi_{\mathbf{k}}^2}{E_{\mathbf{k}}^3}. \end{aligned} \quad (34)$$

At finite T , the AB mode becomes damped, and the real and imaginary parts of the sound velocity have to be calculated numerically. Although, the algebra is somewhat complicated, it can be shown that the AB mode satisfies $c \rightarrow 0$ as $T \rightarrow T_c$, as expected.

To include the amplitude renormalization, using Eq. (12b), we can write

$$\begin{aligned} q_\mu K_0^{\mu\nu} q_\nu &= q_\mu K_0^{\mu\nu} q_\nu - \frac{q_\mu R^{\mu 1} R^{1\nu} q_\nu}{\tilde{Q}_{11}} \\ &\approx q_\mu K_0^{\mu\nu} q_\nu - \Omega^2 \frac{R^{01} R^{10}}{\tilde{Q}_{11}}, \end{aligned} \quad (35)$$

where in the second line, we have used the $T=0$ approximation for the second term, so that $R^{i1}(0) = 0 = R^{1i}(0)$ for $i = 1, 2, 3$, $\tilde{Q}_{11}(0) = 2|g| - \alpha_{11}$, and

$$R^{10}(0) = R^{01}(0) = -\Delta_{sc} \sum_{\mathbf{k}} \frac{\epsilon_{\mathbf{k}}}{E_{\mathbf{k}}^3} \varphi_{\mathbf{k}}^2. \quad (36)$$

This greatly simplifies the numerical calculations.

It should be noted that the temperature dependence of the amplitude contribution is always suppressed by the Fermi function $f(E_{\mathbf{k}})$. This amplitude renormalization is negligible at weak coupling strengths, where the T dependence may be strong near T_c due to the small size of the gap. On the other hand, when the coupling strength increases, and thus amplitude effects become more important, the excitation gap becomes large for all $T \leq T_c$. This follows as a result of pseudogap effects. Hence, the amplitude contribution is rather insensitive to T . Therefore, it is reasonable, in both the strong and weak coupling cases, to neglect the T dependence of the amplitude contribution in the numerical analysis.

V. NUMERICAL RESULTS: ZERO AND FINITE TEMPERATURES

In this section we summarize numerical results obtained for the AB mode velocity c associated with the electromagnetic response kernel, as obtained by solving Eqs. (18) and

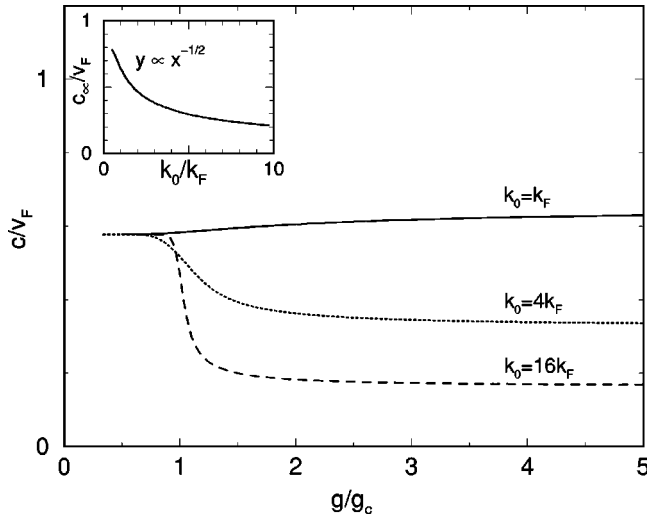


FIG. 4. AB mode velocity c/v_F as a function of the coupling strength (main figure) for various densities characterized by k_0/k_F in 3D jellium. Plotted in the inset is the large g asymptote c_∞/v_F , versus k_0/k_F , which varies as $(k_F/k_0)^{1/2}$, as expected.

(19). We also briefly discuss the behavior for the $T=0$ phase mode velocity v_ϕ that results from the coupling to density fluctuations, as well [see Eq. (23)]. The former, which has physical implications for the behavior of the dielectric constant,^{44,41} is the more straightforward to compute, because it does not require any new approximations associated with the effective interactions V in the particle-hole channel. The analysis of this section provides information about the nature of the “quasi-ideal” Bose gas limit, which we address via plots of the infinite g asymptote of the AB mode, called c_∞ . It also helps to clarify how pair fluctuations contribute, at finite temperatures, to the collective mode dispersion. Our $T=0$ calculations are based on the Leggett ground state which corresponds to that of the pairing approximation as well. At finite T , we numerically evaluate the AB sound dispersion from Eq. (33), obtained within the framework of the pairing approximation.

In Fig. 4 we plot the zero-temperature value of c as a function of the dimensionless coupling strength g/g_c , where $g_c = -4\pi/mk_0$ is the critical value of the coupling above which bound pairs are formed in vacuum. Here we consider a 3D jellium model (with $\varphi_k = [1 + (k/k_0)^2]^{-1/2}$) at three different electron densities, which are parametrized via k_0/k_F . The most interesting feature of these and related curves is shown in the inset where we plot the asymptotic limit for each value of density or, equivalently, k_0 . This numerically obtained asymptote reflects the *effective* residual boson-boson interactions in the “quasi-ideal” Bose gas limit and is close to the value calculated in Ref. 39 whose functional dependence is given by $c_\infty/v_F \propto \sqrt{k_F/k_0}$ or, equivalently, $c_\infty \propto \sqrt{n/k_0}$. Interpreting the physics as if the system were a true interacting Bose system, one would obtain the effective interaction $U(0) \approx 3\pi^2/mk_0$, independent of g in the strong coupling limit. As expected, these interboson interactions come exclusively from the underlying fermion character of the system, and can be associated with the repulsion between the fermions due to the Pauli principle. All of this is seen most directly^{8,15,14} by noting that the behavior displayed in the inset can be interpreted in terms of the ef-

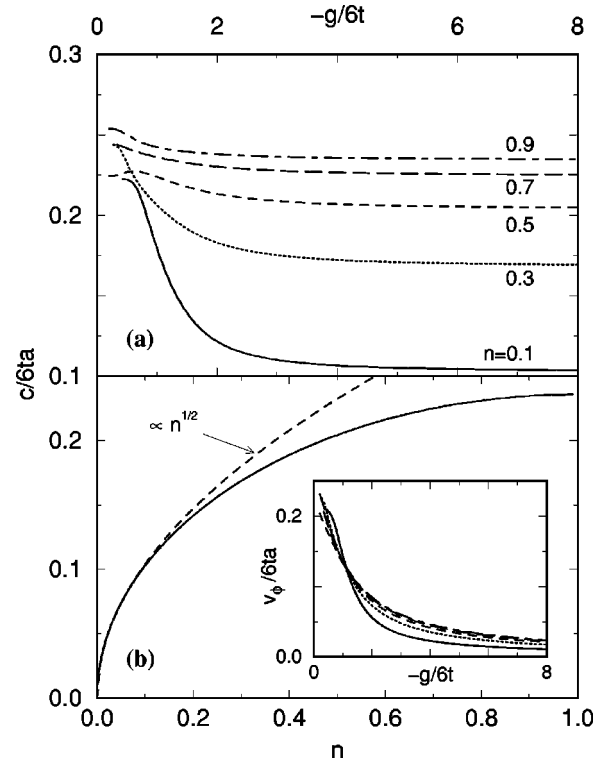


FIG. 5. (a) Normalized AB mode velocity, $c/6ta$, on a 3D lattice with an s -wave pairing interaction for various densities as a function of g , and (b) the large g limit for $c/6ta$ as a function of density n for fixed $-g/6t = 20$. (Here $6t$ is the half bandwidth.) The dashed line in (b) shows a fit to the expected low density dependence $n^{1/2}$. Plotted in the inset is the velocity of the phase and density coupled collective mode $v_\phi/6ta$ with the particle-hole channel treated at the RPA level, for the same n as in (a).

fective scattering length of the bosons a_B , which is found to be twice that of the fermions a_F in the strong coupling limit. Effects associated with the coupling constant g are, thus, entirely incorporated into making bosons out of a fermion pair, and are otherwise invisible.

The same calculations are repeated in Fig. 5 for a tight binding lattice band structure with $\varphi_k = 1$ at $T=0$. Figure 5(a) plots the sound velocity for different densities n , as a function of the coupling constant; the behavior of the large g limit is shown in Fig. 5(b) as a function of density for a fixed g . Near half filling, where there is particle-hole symmetry, the amplitude contributions are irrelevant and the large g limit for c , from Eq. (34), is $c = \sqrt{2}t$, where t is the hopping integral. At low n the AB velocity varies as \sqrt{n} , which is consistent with the results shown above for jellium. In both cases the behavior again reflects the underlying fermionic character, since it is to be associated with a Pauli principle induced repulsion between bosons. Unlike in the jellium case, where c approaches a finite asymptote as g increases, here c vanishes asymptotically due to the increase of the pair mass associated with lattice effects.^{21,19} For completeness, we also show, as an inset in Fig. 5(b), the behavior of v_ϕ , where we have used the RPA approximation to characterize the parameter V in the particle-hole channel. This approximation is in the spirit of previous work by Belkhir and Randeria,³⁴ although it cannot be readily motivated at sufficiently large g .

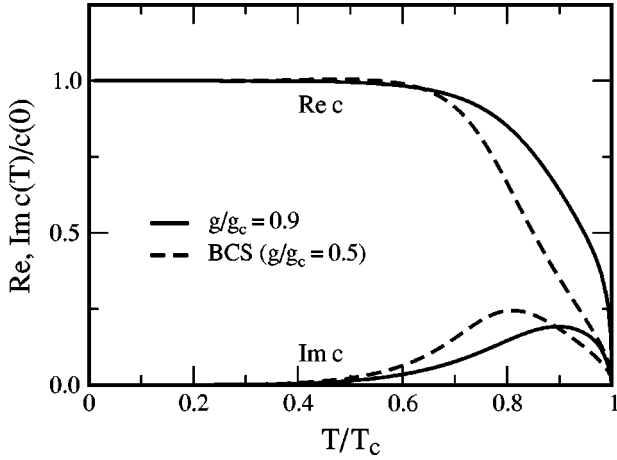


FIG. 6. Temperature dependence of the real ($\text{Re } c$) and imaginary ($\text{Im } c$) parts of the AB mode velocity for moderate coupling (solid lines) and weak coupling BCS (dashed lines) in 3D jellium with $k_0 = 4k_F$. The mode is highly damped as T_c is approached.

Finally, in Fig. 6 we plot the temperature dependence of the AB mode velocity (both real and imaginary parts), for moderately strong coupling (solid lines) and the BCS limit (dashed lines). This figure suggests that the AB mode velocity reflects the same transition temperature T_c as is computed via the excited pair propagator or T matrix. This represents an important self-consistency check on the present formalism.

VI. CONCLUSIONS

This paper deals with the fairly complex issues of pair fluctuations, collective modes, and gauge invariance in a BCS Bose-Einstein crossover scenario. A starting point for our approach is the Leggett ground state, which imposes rather strong constraints on the nature of the physics of fermions and composite bosons. The fermion degrees of freedom are always present through the self consistency conditions. Not only are these fermion pairs different from true bosons, but they represent a very special type of composite boson which can be associated with the underlying structure of the BCS state. Even at $T=0$ one can see from previous work on the BCS-BEC crossover, that these constraints lead to a mix of ideal Bose gas¹⁸ and nonideal³⁴ Bose liquid behavior. This mirrors some of the effects of BCS theory, in which the system undergoes a form of Bose condensation with a *full* condensate fraction $n_0/n = 1$, at $T=0$. Nevertheless, a BCS superconductor has a soundlike collective (phase) mode that is intimately associated with its superconductivity. At a more technical level, it is instructive to contrast the polarizability associated with the phase mode, called $Q'_{22}(Q)$ in the present paper, with the pair susceptibility which we call $\chi(Q)$. These two modes correspond to distinct dynamical branches, although both become soft at $\mathbf{q}=\mathbf{0}$ under the same conditions. The softness of the former is naturally associated with the Goldstone boson and the latter with a vanishing chemical potential for pairs: $\mu_{\text{pair}}=0$.

A central physics theme of this paper is reflected in Fig. 1. The crossover problem introduces an important new parameter Δ_{pg} , which characterizes the excited states of a non-BCS superconductor. As a result, there are three coupled

equations [Eqs. (4)] to be satisfied for Δ_{pg} , Δ , and μ , at finite T , in contrast to zero-temperature crossover theories where there are only two. This new parameter is a measure of the difference between the excitation gap and the superconducting order parameter. One can also arrive at a picture that is similar to Fig. 1 within the phase fluctuation scenario.³ What is different here is the ‘‘tuning parameter,’’ which corresponds to the coupling strength g in the crossover picture, and the phase stiffness parameter in the phase fluctuation picture.

One may summarize our results by asking the following series of questions, which our paper raises and answers.

Is there any precedent for soft modes other than Goldstone bosons? Yes. In the present paper we find that a vanishing value for the pair chemical potential μ_{pair} below T_c leads to a soft mode for incoherent, finite momentum pair excitations. These excitations are analogous to the ‘‘particle’’ excitations in the case of the neutral Bose liquid. Moreover, for the Bose liquid, this branch is also soft and always different (except at strictly zero wavevector) from the Goldstone boson. However, in the true Bose system the two branches have the same slope at $\mathbf{q}=\mathbf{0}$.

Should the T matrix \mathcal{T} be renormalized so as to yield the sound mode dispersion at small wave-vectors, as in a Bose liquid? With this renormalization \mathcal{T} would then be similar to its Bose liquid counterpart³⁸ and in this way the pair excitation dispersion $\Omega_{\mathbf{q}}$ at small wave vectors would be linear in \mathbf{q} , rather than quadratic as we have found. We answer this question by noting that the fermion degrees of freedom strongly constrain \mathcal{T} so that the composite boson system is different from the Bose liquid. As a consequence, the proposed renormalization seems problematical. (i) Adding in this collective mode effect associated with the Bose liquid is equivalent to including boson-boson interactions. In the present composite boson case, these boson-boson interactions derive from fermionic degrees of freedom, i.e., the Pauli principle, which has already been accounted for in our calculations of \mathcal{T} . It is not clear why these boson-boson interactions should then be included yet a second time. (ii) Once there is a renormalization of \mathcal{T} , this will change the ground state gap equation and corresponding constraint on the fermionic chemical potential μ . (iii) Finally, this renormalization will introduce an unphysical incomplete condensation in the ground state, like its counterpart in the Bose liquid.

What about the significance of Coulomb renormalizations of the pair propagator? If Coulomb interactions were included, presumably, the pair fluctuation mode would then be gapped. This would again compromise the self-consistent conditions on Δ and μ in the ground state. Indeed, within the BCS formalism (as well as in the Leggett ground state) long range Coulomb interactions do not enter in an important way to change the gap equation structure, but rather they principally affect the collective modes. It is for this reason that we argued earlier that Coulomb effects are presumed to be already included in the pairing interaction. Indeed, at large g , we have seen that essentially all signs of the two-body (g dependent) fermion-fermion interaction are absent in the effective boson-boson interaction, which is deduced from the sound mode velocity.

Does this paper in any way change the way we think about BCS theory? Absolutely not. BCS theory appears as a

special case in the weak coupling g , particle-hole symmetric limit of the more general approach. When we study pair excitations in this limit, we find they are greatly damped at all wave vectors q , and it makes no sense to talk about them. In this way $\Delta_{pg}(T_c)/\Delta_{sc}(0)$ is vanishingly small in the BCS limit.

To what extent are the results of this paper limited by the T -matrix approximation? The T -matrix approximation seems to be intimately connected to the physics of the crossover scenario. This scheme represents, in some sense, a truncation of the interactions at a pairwise level. This truncation, which appears to generate a quasi-ideal Bose gas character to the composite boson system, mirrors the behavior of the well established ground state. This approach might not be suitable for other composite boson scenarios, which do not evolve directly from the BCS phase. Nevertheless, these crossover schemes provide a useful way of learning about composite boson systems in general. Moreover, they provide valuable insights about how to extend BCS theory slightly, without abandoning it altogether, and in this way to address a large class of short coherence length, but otherwise conventional, superconductors.

ACKNOWLEDGMENTS

We are very grateful to A. J. Leggett, G. F. Mazenko, A. A. Varlamov, and P. B. Wiegmann for useful discussions and to I. O. Kulik for helpful communications. This work was supported by grants from the National Science Foundation through the Science and Technology Center for Superconductivity under Grant No. DMR 91-20000 and through the MRSEC under Grant No. DMR 9808595, 5-43030.

APPENDIX A: SELF-CONSISTENT T -MATRIX APPROXIMATIONS—GENERAL RESULTS FOR THE SUPERCONDUCTING PHASE

In this appendix we present the self consistency conditions and related gap equations associated with the superconducting state within the broad class of T -matrix-based crossover theories. An important goal of this discussion is to show that Eqs. (1)–(3) are rather general consequences of these schemes when applied below T_c . We show in addition how to derive Eqs. (4) within the pairing approximation.¹¹ In these general schemes one solves three coupled equations for the self-energy $\Sigma(K)$, T matrix (or pair propagator) $\mathcal{T}(Q)$, and chemical potential μ :

$$\Sigma(K) = G_0^{-1}(K) - G^{-1}(K) = \sum_Q \mathcal{T}(Q) \tilde{G}(Q-K) \varphi_{\mathbf{k}-\mathbf{q}/2}^2, \quad (\text{A1a})$$

$$g = [1 + g \chi(Q)] \mathcal{T}(Q), \quad (\text{A1b})$$

$$n = 2 \sum_K G(K). \quad (\text{A1c})$$

The choice of the functions \tilde{G} and pair susceptibility χ varies from one approximation to another. The FLEX (or GG) approximation^{16,37,27} takes $\tilde{G} = G$, so that $\chi(Q) = \chi^{FLEX}(Q) = \sum_K G(K) G(Q-K) \varphi_{\mathbf{k}-\mathbf{q}/2}^2$ and $\Sigma(K) = \Sigma^{FLEX}(K)$

$= \sum_P \mathcal{T}(P) G(P-K) \varphi_{\mathbf{k}-\mathbf{p}/2}^2$. On the other hand, the pairing approximation^{11,12} (or GG_0 scheme) sets $\tilde{G} = G_0$, so that $\chi(Q) = \chi^{pair}(Q) = \sum_K G(K) G_0(Q-K) \varphi_{\mathbf{k}-\mathbf{q}/2}^2$ and $\Sigma(K) = \Sigma^{pair}(K) = \sum_P \mathcal{T}(P) G_0(P-K) \varphi_{\mathbf{k}-\mathbf{p}/2}^2$. As the temperature is lowered toward T_c , the T matrix develops a divergence at $Q=0$, and the transition to the broken symmetry phase is signaled by a pole given by

$$g T^{-1}(Q=0; T_c) = 1 + g \chi(Q=0; T_c, \Delta) = 0. \quad (\text{A2})$$

The counterpart of this analysis is considerably more complicated below T_c . The procedure, which we summarize in this section, is an approximation which is chosen to satisfy the following four criteria: (i) It leads to the same transition temperature when approached from below as from above. (ii) It leads directly to a *physical* interpretation of the BCS-BEC crossover scheme as discussed in Sec. II and illustrated in Fig. 1. An important, and third criterion which we view as an additional check on the approximations used is that (iii) one should recover the BCS scheme in weak coupling for all $T \leq T_c$ and, finally, (iv) one should recover the Leggett ground state at $T=0$.

Assuming that the T matrix acquires a singular delta-function component, which describes the ($Q=0$) Cooper pair condensate in equilibrium, we write

$$\mathcal{T}(Q) = \mathcal{T}_{sc}(Q) + \mathcal{T}_{pg}(Q), \quad (\text{A3})$$

where $\mathcal{T}_{sc}(Q) = -(\Delta_{sc}^2/T) \delta(Q)$ and $\mathcal{T}_{pg}(Q) = g/[1 + g \chi(Q)]$. One arrives at the following general gap equation:

$$1 + g \chi(Q=0; T, \Delta) = 0, \quad T \leq T_c. \quad (\text{A4})$$

Setting $\Delta_{sc}=0$ at T_c leads back to Eq. (A2), the same gap equation as obtained by approaching T_c from above. As a consequence of Eq. (A4), the regular part of the T matrix $\mathcal{T}_{pg}(Q)$ diverges as $Q \rightarrow 0$; it can be written in the form

$$\mathcal{T}_{pg}(i\Omega, q) = a_0 / (i\Omega - \Omega_q + i\Gamma_q), \quad T \leq T_c \quad (\text{A5})$$

in accord with Eq. (1). Here $\Gamma_q \rightarrow 0$ as $\mathbf{q} \rightarrow \mathbf{0}$. The self-energy of Eq. (A1a) may be decomposed into two terms:

$$\Sigma(K) = \Sigma_{sc}(K) + \Sigma_{pg}(K), \quad (\text{A6})$$

where the term associated with the condensate contribution (\mathcal{T}_{sc}) is

$$\Sigma_{sc}(K) = -\Delta_{sc}^2 \varphi_{\mathbf{k}}^2 \tilde{G}(-K). \quad (\text{A7})$$

In evaluating the pseudogap contribution (\mathcal{T}_{pg}) to Σ , as a consequence of Eq. (A4), the main contribution to the Q sum comes from the small Q region, so that the integral may be approximated by

$$\Sigma_{pg}(K) \approx \tilde{G}(-K) \varphi_{\mathbf{k}}^2 \sum_Q \mathcal{T}_{pg}(Q) = -\Delta_{pg}^2 \varphi_{\mathbf{k}}^2 \tilde{G}(-K). \quad (\text{A8})$$

In this way the total self-energy is

$$\Sigma(K) \approx -\Delta^2 \varphi_{\mathbf{k}}^2 \tilde{G}(-K), \quad \Delta \equiv \sqrt{\Delta_{sc}^2 + \Delta_{pg}^2}. \quad (\text{A9})$$

The above discussion is expected to apply to both the FLEX scheme and the pairing approximation. Moreover, on the basis of the behavior above T_c , there is no *a priori* reason to select one approach over the other. However, the latter seems to be preferred if one imposes the third and fourth criteria discussed above.

If we adopt the pairing approximation, so that $\tilde{G} = G_0$, the BCS gap equation (in the absence of pseudogap) follows from Eq. (A4):

$$1 + g \sum_Q G(K) G_0(-K) = 1 + g \sum_K \frac{\Delta_{sc}^2 \varphi_{\mathbf{k}}^2}{\omega^2 + E_{\mathbf{k}}^2} = 0. \quad (\text{A10})$$

In a similar way, the entire set of three equations associated with the pairing approximation¹¹ [Eqs. (4) in Sec. II B] can be readily obtained.

An additional check on the validity of the approximation scheme relates to criterion (iv), we note that, as a consequence of the Bose function $b(\Omega)$ in Eq. (3), quite generally $\lim_{T \rightarrow 0} \Delta_{pg} = 0$, as is consistent with a physical picture in which Δ_{pg} is associated with classical fluctuations. Therefore, within the pairing approximation, the resulting ground state [see Eqs. (4a) and (4b)] is the same as that proposed by Leggett.¹⁸

APPENDIX B: EVALUATION OF THE VERTEX CORRECTIONS

In this appendix we demonstrate an explicit cancellation between the Maki-Thompson (MT) and Aslamazov-Larkin (AL) diagrams of Fig. 3. In this way we prove that the contribution to the vertex correction $\delta\Lambda$ from the superconducting order parameter is given by the Maki-Thompson diagram, and the pseudogap contribution $\delta\Lambda_{pg}$ comes from MT and AL diagrams. It is easy to demonstrate a cancellation between the MT diagram and the AL diagrams, which will greatly simplify the calculations. In general, we have

$$\begin{aligned} & \delta\Lambda_{pg}^\mu(K, K-Q) q_\mu \\ &= -(MT)_{pg} + \sum_P \mathcal{T}_{pg}(P) G_0(P-K) \frac{\partial \varphi_{\mathbf{k}-\mathbf{p}/2-\mathbf{q}/2}^2}{\partial \mathbf{k}} \cdot \mathbf{q}, \end{aligned} \quad (\text{B1})$$

where $(MT)_{pg}$ refers to the MT diagram contribution, and $\mathcal{T}_{pg}(Q \neq 0)$ is the T matrix or pair propagator.

To prove this cancellation, we notice that the vertex corrections in the (four-)current-current correlation functions can be obtained from proper vertex insertions in the single particle Green's functions in the self-energy diagram. In the pairing approximation (G_0G scheme) we have

$$\Sigma_{pg}(K) = \sum_L \mathcal{T}_{pg}(K+L) G_0(L) \varphi_{(K-L)/2}^2, \quad (\text{B2})$$

where L is the four-momentum of the fermion loop, this procedure leads to one Maki-Thompson diagram and two Aslamazov-Larkin diagrams.

Obviously, L in Eq. (B2) is a dummy variable so that its variation does not change $\Sigma(K)$, namely,

$$\begin{aligned} 0 &= \sum_L [\mathcal{T}_{pg}(K+L+\Delta L) G_0(L+\Delta L) \varphi_{(K-L-\Delta L)/2}^2 \\ &\quad - \mathcal{T}_{pg}(K+L) G_0(L) \varphi_{(K-L)/2}^2] \\ &= \sum_L \{ [\mathcal{T}_{pg}(K+L+\Delta L) - \mathcal{T}_{pg}(K+L)] \\ &\quad \times G_0(L+\Delta L) \varphi_{(K-L-\Delta L)/2}^2 + \mathcal{T}_{pg}(K+L) \\ &\quad \times [G_0(L+\Delta L) - G_0(L)] \varphi_{(K-L-\Delta L)/2}^2 + \mathcal{T}_{pg}(K+L) \\ &\quad \times G_0(L) [\varphi_{(K-L-\Delta L)/2}^2 - \varphi_{(K-L)/2}^2] \} \end{aligned} \quad (\text{B3})$$

Using $G(K)G^{-1}(K) = 1$, we obtain

$$\begin{aligned} & G(K+\Delta K) - G(K) \\ &= -G(K) [G^{-1}(K+\Delta K) - G^{-1}(K)] G(K+\Delta K) \\ &= -G(K) \Lambda_\mu(K+\Delta K, K) G(K) \Delta K^\mu, \end{aligned} \quad (\text{B4a})$$

where $G^{-1}(K+\Delta K) - G^{-1}(K) \approx \Lambda_\mu(K+\Delta K, K) \Delta K^\mu$ is the full vertex. Similarly, we have

$$\begin{aligned} & G_0(K+\Delta K) - G_0(K) \\ &= -G_0(K) [G_0^{-1}(K+\Delta K) - G_0^{-1}(K)] G_0(K+\Delta K) \\ &= -G_0(K) \lambda_\mu(K+\Delta K, K) G_0(K) \Delta K^\mu, \end{aligned} \quad (\text{B4b})$$

where $G_0^{-1}(K+\Delta K) - G_0^{-1}(K) \approx \lambda_\mu(K+\Delta K, K) \Delta K^\mu$ is the bare vertex, and $\lambda^\mu(K+\Delta K, K) = (1, \nabla_{\mathbf{k}} \epsilon_{\mathbf{k}+\Delta \mathbf{k}/2})$. Equations (B4a) correspond to the vertex insertions diagrammatically along the full and bare Green's functions, respectively.

Using $\mathcal{T}_{pg}(K+L) = g/[1 + g\chi(K+L)]$, we obtain

$$\begin{aligned} & \mathcal{T}_{pg}(K+L+\Delta L) - \mathcal{T}_{pg}(K+L) \\ &= -\mathcal{T}_{pg}(K+L+\Delta L) [\chi(K+L+\Delta L) \\ &\quad - \chi(K+L)] \mathcal{T}_{pg}(K+L). \end{aligned} \quad (\text{B5})$$

Writing $\chi(K+L) = \sum_{L'} G(L') G_0(K+L-L') \varphi_{L'-(K+L)/2}^2$, we have

$$\begin{aligned} & \chi(K+L+\Delta L) - \chi(K+L) \\ &= \sum_{L'} G(L') \{ [G_0(K+L-L'+\Delta L) \\ &\quad - G_0(K+L-L')] \varphi_{L'-(K+L+\Delta L)/2}^2 + G_0(K+L-L') \\ &\quad \times [\varphi_{L'-(K+L+\Delta L)/2}^2 - \varphi_{L'-(K+L)/2}^2] \}. \end{aligned} \quad (\text{B6})$$

On the other hand, writing $\chi(K+L) = \sum_{L'} G(K+L-L') G_0(L') \varphi_{(K+L)/2-L'}^2$, we get

$$\begin{aligned}
& \chi(K+L+\Delta L) - \chi(K+L) \\
&= \sum_{L'} \{ [G(K+L-L'+\Delta L) - G(K+L-L')] \\
&\quad \times G_0(L') \varphi_{(K+L+\Delta L)/2-L'}^2 + G(L') G_0(K+L-L') \\
&\quad \times [\varphi_{L'-(K+L-\Delta L)/2}^2 - \varphi_{L'-(K+L)/2}^2] \}. \quad (\text{B7})
\end{aligned}$$

Combining Eq. (B6) and Eq. (B7), we obtain to the first order of ΔL

$$\begin{aligned}
& \chi(K+L+\Delta L) - \chi(K+L) \\
&= \frac{1}{2} \sum_{L'} \{ G(L') [G_0(K+L-L'+\Delta L) \\
&\quad - G_0(K+L-L')] \varphi_{L'-(K+L+\Delta L)/2}^2 \\
&\quad + [G(K+L-L'+\Delta L) - G(K+L-L')] \\
&\quad \times G_0(L') \varphi_{L'-(K+L+\Delta L)/2}^2 \}, \quad (\text{B8})
\end{aligned}$$

where we have assumed in general $\varphi_K^2 = \varphi_{-K}^2$. Substituting Eq. (B8) and Eq. (B5) into Eq. (B3), we obtain

$$\begin{aligned}
0 &= -\frac{1}{2} \sum_{LL'} \mathcal{T}_{pg}(K+L+\Delta L) \mathcal{T}_{pg}(K+L) \{ G(L') [G_0(K+L \\
&\quad - L'+\Delta L) - G_0(K+L-L')] \varphi_{L'-(K+L+\Delta L)/2}^2 \\
&\quad + [G(K+L-L'+\Delta L) - G(K+L-L')] \\
&\quad \times G_0(L') \varphi_{L'-(K+L+\Delta L)/2}^2 \} G_0(L+\Delta L) \varphi_{(K-L-\Delta L)/2}^2 \\
&\quad + \sum_L \mathcal{T}_{pg}(K+L) [G_0(L+\Delta L) - G_0(L)] \varphi_{(K-L-\Delta L)/2}^2 \\
&\quad + \sum_L \mathcal{T}_{pg}(K+L) G_0(L) [\varphi_{(K-L-\Delta L)/2}^2 - \varphi_{(K-L)/2}^2]. \quad (\text{B9})
\end{aligned}$$

Comparing this with the analytical expressions corresponding to the diagrams in Fig. 3, it is easy to identify the first two terms as the two AL diagrams (which we denote by AL_1 and AL_2) and the third one with the MT diagram for the pseudogap vertex corrections. Therefore,

$$\begin{aligned}
& \frac{1}{2} [(AL_1) + (AL_2)] + (MT)_{pg} + \sum_L \mathcal{T}_{pg}(K+L) G_0(L) \\
&\quad \times [\varphi_{(K-L-\Delta L)/2}^2 - \varphi_{(K-L)/2}^2] = 0. \quad (\text{B10})
\end{aligned}$$

Finally, we have

$$\begin{aligned}
& \delta\Lambda_{pg}^\mu(K, K-\Delta L) \Delta L_\mu = (AL_1) + (AL_2) + (MT)_{pg} \\
&= -(MT)_{pg} - 2 \sum_L \mathcal{T}_{pg}(K+L) G_0(L) \\
&\quad \times \frac{\partial \varphi_{(K-L-\Delta L)/2}^2}{\partial L} \Delta L. \quad (\text{B11})
\end{aligned}$$

Changing variables $K+L \rightarrow P, \Delta L \rightarrow Q$ leads to Eq. (B1).

The two contributions which enter Eq. (32) result from adding the superconducting gap and pseudogap terms, which are given, respectively, by

$$\begin{aligned}
& \delta\Lambda_{sc}(K, K-Q) = -\Delta_{sc}^2 \varphi_{\mathbf{k}} \varphi_{\mathbf{k}-\mathbf{q}} G_0(-K) G_0(Q-K) \\
&\quad \times \lambda(Q-K, -K), \quad (\text{B12a})
\end{aligned}$$

and

$$\begin{aligned}
& \delta\Lambda_{pg}^\mu(K, K-Q) = -\sum_P \mathcal{T}_{pg}(P) \varphi_{\mathbf{k}-\mathbf{p}/2} \varphi_{\mathbf{k}-\mathbf{q}-\mathbf{p}/2} G_0(P-K) \\
&\quad \times G_0(P+Q-K) \lambda^\mu(P+Q-K, P-K) \\
&\quad + \sum_P \mathcal{T}_{pg}(P) G_0(P-K) \frac{\partial \varphi_{\mathbf{k}-\mathbf{p}/2-\mathbf{q}/2}^2}{\partial k_\mu}, \quad (\text{B12b})
\end{aligned}$$

APPENDIX C: FULL EXPRESSIONS FOR THE CORRELATION FUNCTIONS $\vec{\mathbf{P}}$, \mathbf{P}_0 , AND P_{00}

It is useful here to write down the component contributions to the different correlation functions in the electromagnetic response. After adding the superconducting and pseudogap contributions one finds for the current-current correlation function

$$\begin{aligned}
\frac{\vec{\mathbf{n}}}{\mathbf{m}} + \vec{\mathbf{P}} &= 2 \sum_{\mathbf{k}} \frac{\Delta_{sc}^2}{E_{\mathbf{k}}^2} \left[\frac{1-2f(E_{\mathbf{k}})}{2E_{\mathbf{k}}} + f'(E_{\mathbf{k}}) \right] \left[\varphi_{\mathbf{k}}^2 (\nabla \epsilon_{\mathbf{k}}) (\nabla \epsilon_{\mathbf{k}}) \right. \\
&\quad \left. - \frac{1}{4} (\nabla \epsilon_{\mathbf{k}}^2) (\nabla \varphi_{\mathbf{k}}^2) \right] \\
&\quad - 2 \sum_{\mathbf{k}} f'(E_{\mathbf{k}}) \frac{\Omega^2}{\Omega^2 - (\mathbf{q} \cdot \nabla E_{\mathbf{k}})^2} (\nabla \epsilon_{\mathbf{k}}) (\nabla \epsilon_{\mathbf{k}}) \\
&\quad + \sum_{\mathbf{k}} \frac{\Delta_{pg}^2}{E_{\mathbf{k}}^2} f'(E_{\mathbf{k}}) \frac{\Omega^2}{\Omega^2 - (\mathbf{q} \cdot \nabla E_{\mathbf{k}})^2} \left[\varphi_{\mathbf{k}}^2 (\nabla \epsilon_{\mathbf{k}}) (\nabla \epsilon_{\mathbf{k}}) \right. \\
&\quad \left. - \frac{1}{4} (\nabla \epsilon_{\mathbf{k}}^2) (\nabla \varphi_{\mathbf{k}}^2) \right], \quad (\text{C1})
\end{aligned}$$

and for the current-density correlation function

$$\mathbf{P}_0 = -2\Omega \sum_{\mathbf{k}} \frac{\epsilon_{\mathbf{k}}}{E_{\mathbf{k}}} f'(E_{\mathbf{k}}) \frac{\mathbf{q} \cdot \nabla E_{\mathbf{k}}}{\Omega^2 - (\mathbf{q} \cdot \nabla E_{\mathbf{k}})^2} \nabla \epsilon_{\mathbf{k}}, \quad (\text{C2})$$

and finally for the density-density correlation function

$$P_{00} = -2 \sum_{\mathbf{k}} \frac{\Delta_{sc}^2 \varphi_{\mathbf{k}}^2}{E_{\mathbf{k}}^2} \left[\frac{1 - 2f(E_{\mathbf{k}})}{2E_{\mathbf{k}}} + f'(E_{\mathbf{k}}) \right] + 2 \sum_{\mathbf{k}} f'(E_{\mathbf{k}}) \frac{\Omega^2 \Delta_{sc}^2 \varphi_{\mathbf{k}}^2 - E_{\mathbf{k}}^2 (\mathbf{q} \cdot \nabla E_{\mathbf{k}})^2}{E_{\mathbf{k}}^2 [\Omega^2 - (\mathbf{q} \cdot \nabla E_{\mathbf{k}})^2]}. \quad (\text{C3})$$

In deriving the first of these we have integrated by parts to evaluate

$$\frac{n}{m} = 2 \sum_{\mathbf{k}} \frac{\partial^2 \epsilon_{\mathbf{k}}}{\partial \mathbf{k} \partial \mathbf{k}} G(K)$$

$$= -2 \sum_{\mathbf{k}} G^2(K) (\nabla \epsilon_{\mathbf{k}}) \cdot [\nabla \epsilon_{\mathbf{k}} + \nabla \Sigma(K)]$$

$$= 2 \sum_{\mathbf{k}} \frac{\Delta^2}{E_{\mathbf{k}}^2} \left[\frac{1 - 2f(E_{\mathbf{k}})}{2E_{\mathbf{k}}} + f'(E_{\mathbf{k}}) \right] \left[\varphi_{\mathbf{k}} (\nabla \epsilon_{\mathbf{k}}) \cdot (\nabla \epsilon_{\mathbf{k}}) \right.$$

$$\left. - \frac{1}{4} (\nabla \epsilon_{\mathbf{k}})^2 \cdot (\nabla \varphi_{\mathbf{k}}^2) \right] - 2 \sum_{\mathbf{k}} f'(E_{\mathbf{k}}) (\nabla \epsilon_{\mathbf{k}}) \cdot (\nabla \epsilon_{\mathbf{k}}). \quad (\text{C4})$$

These expressions are then used to evaluate Eq. (33) in the text.

- ¹H. Ding, T. Yokoya, J. C. Campuzano, T. Takahashi, M. Randeria, M. R. Norman, T. Mochiku, K. Hadowaki, and J. Giapintzakis, *Nature (London)* **382**, 51 (1996).
- ²A.G. Loeser, Z.-X. Shen, D. S. Dessau, D. S. Marshall, C. H. Park, P. Fournier, and A. Kapitulni, *Science* **273**, 325 (1996).
- ³V.J. Emery and S.A. Kivelson, *Nature (London)* **374**, 434 (1995).
- ⁴M. Franz and A.J. Millis, *Phys. Rev. B* **58**, 14 572 (1998).
- ⁵P.A. Lee and X.G. Wen, *Phys. Rev. Lett.* **78**, 4111 (1997).
- ⁶M. Randeria, J.-M. Duan, and L.-Y. Shieh, *Phys. Rev. Lett.* **62**, 981 (1989); *Phys. Rev. B* **41**, 327 (1990).
- ⁷R. Micnas, M. H. Pedersen, S. Schafroth, T. Schneider, J. J. Rodriguez-Nunez, and H. Beck, *Phys. Rev. B* **52**, 16 223 (1995).
- ⁸R. Haussmann, *Z. Phys. B: Condens. Matter* **91**, 291 (1993).
- ⁹B. Jankó, J. Maly, and K. Levin, *Phys. Rev. B* **56**, 11 407 (1997).
- ¹⁰Y.J. Uemura *et al.*, *Phys. Rev. Lett.* **62**, 2317 (1989); Y.J. Uemura, *Physica C* **282**, 194 (1997).
- ¹¹I. Kosztin, Q.J. Chen, B. Jankó, and K. Levin, *Phys. Rev. B* **58**, R5936 (1998).
- ¹²Q.J. Chen, I. Kosztin, B. Jankó, and K. Levin, *Phys. Rev. Lett.* **81**, 4708 (1998).
- ¹³J. Maly, B. Jankó, and K. Levin, *Phys. Rev. B* **59**, 1354 (1999); *Physica C* **321**, 113 (1999).
- ¹⁴M. Drechsler and W. Zwerger, *Ann. Phys. (Leipzig)* **1**, 15 (1992).
- ¹⁵C.A.R. Sá de Melo, M. Randeria, and J.R. Engelbrecht, *Phys. Rev. Lett.* **71**, 3202 (1993).
- ¹⁶O. Tchernyshyov, *Phys. Rev. B* **56**, 3372 (1997).
- ¹⁷J. Ranninger and J.M. Robin, *Phys. Rev. B* **53**, 11 961 (1996).
- ¹⁸A.J. Leggett, *J. Phys. (Paris), Colloq.* **41**, C7-19 (1980); also in *Modern Trends in the Theory of Condensed Matter*, edited by A. Pekalski and J. Przystawa, Lecture Notes in Physics No. 115 (Springer, Berlin, 1980).
- ¹⁹Q.J. Chen, I. Kosztin, B. Jankó, and K. Levin, *Phys. Rev. B* **59**, 7083 (1999).
- ²⁰D.M. Eagles, *Phys. Rev.* **186**, 456 (1969).
- ²¹P. Nozières and S. Schmitt-Rink, *J. Low Temp. Phys.* **59**, 195 (1985).
- ²²M. Randeria, cond-mat/9710223 (unpublished); in *Bose-Einstein Condensation*, edited by A. Griffin, D.W. Snoke, and S. Stringari (Cambridge University Press, Cambridge, England, 1995), pp. 355-392.
- ²³R. Micnas, J. Ranninger, and S. Robaszkiewicz, *Rev. Mod. Phys.* **62**, 113 (1990).
- ²⁴J.W. Serene, *Phys. Rev. B* **40**, 10 873 (1989).
- ²⁵N. Trivedi and M. Randeria, *Phys. Rev. Lett.* **75**, 312 (1995).
- ²⁶J.M. Singer, M.H. Pedersen, and T. Schneider, *Physica B* **230**, 955 (1997).
- ²⁷J.R. Engelbrecht, A. Nazarenko, M. Randeria, and E. Dagotto, *Phys. Rev. B* **57**, 13 406 (1998).
- ²⁸J.J. Deisz, D.W. Hess, and J.W. Serene, *Phys. Rev. Lett.* **80**, 373 (1998).
- ²⁹N.E. Bickers, D.J. Scalapino, and S.R. White, *Phys. Rev. Lett.* **62**, 961 (1989).
- ³⁰L.P. Kadanoff and P.C. Martin, *Phys. Rev.* **124**, 670 (1961).
- ³¹B.R. Patton, Ph.D. thesis, Cornell University, 1971; *Phys. Rev. Lett.* **27**, 1273 (1971).
- ³²G. Deutscher, *Nature (London)* **397**, 410 (1999).
- ³³Above T_c , the gap equation (4a) no longer holds. Instead, the left-hand side should be equated with a T dependent quantity, τ . Slightly above T_c , this quantity is small $[(T - T_c)]$, therefore, we may still use the approximation given by Eq. (A8). However, the pair excitation spectrum will also acquire a T dependent gap. In consequence, we have a modified set of equations Eqs. (4) to solve for μ , Δ_{pg} , and τ above T_c . This extrapolation becomes worse as T increases. See also Ref. 13.
- ³⁴L. Belkhir and M. Randeria, *Phys. Rev. B* **45**, 5087 (1992).
- ³⁵T. Kostyrko and R. Micnas, *Phys. Rev. B* **46**, 11 025 (1992).
- ³⁶R. Cote and A. Griffin, *Phys. Rev. B* **48**, 10 404 (1993).
- ³⁷R. Haussmann, *Phys. Rev. B* **49**, 12 975 (1994).
- ³⁸A.L. Fetter and J.D. Walecka, *Quantum Theory of Many-Particle Systems* (McGraw-Hill, San Francisco, 1971).
- ³⁹J.R. Engelbrecht, M. Randeria, and C.A.R. Sá de Melo, *Phys. Rev. B* **55**, 15 153 (1997).
- ⁴⁰I.O. Kulik, O. Entin-Wohlman, and R. Orbach, *J. Low Temp. Phys.* **43**, 591 (1981).
- ⁴¹Y.Y. Zha, K. Levin, and D.Z. Liu, *Phys. Rev. B* **51**, 6602 (1995).
- ⁴²P.W. Anderson, *Phys. Rev.* **112**, 1900 (1958).
- ⁴³N.N. Bogoliubov, *Nuovo Cimento* **7**, 794 (1958).
- ⁴⁴R.E. Prange, *Phys. Rev.* **129**, 2495 (1963).
- ⁴⁵R.A. Klemm, K. Scharnberg, D. Walker, and C.T. Rieck, *Z. Phys. B: Condens. Matter* **72**, 139 (1988).
- ⁴⁶J.R. Schrieffer, *Theory of Superconductivity*, 3rd ed. (Benjamin/Cummings, Reading, MA, 1983).
- ⁴⁷A.G. Aronov and V.L. Gurevich, *Zh. Éksp. Teor. Fiz.* **70**, 955 (1976) [*Sov. Phys. JETP* **43**, 498 (1976)].